Annals of Nuclear Medicine Vol. 13, No. 4, 273–276, 1999

Thallium and FDG uptake by atelectasis with bronchogenic carcinoma

Joji KAWABE,* Terue OKAMURA,** Miyuki SHAKUDO,** Koichi KOYAMA,** Hideki WANIBUCHI,*** Yoshihiro SHIMONISHI,** Hironobu OCHI* and Ryusaku YAMADA**

*Division of Nuclear Medicine, **Department of Radiology, and ***First Department of Pathology, Osaka City University Medical School*

We report a case of bronchogenic carcinoma with atelectasis studied by Tl-SPECT and FDG-PET. In the carcinoma, abnormally high uptake of Tl and FDG were detected, but in the region of atelectasis, an abnormally high uptake of Tl with a relatively low uptake of FDG were observed. On quantitative analyses, the Tl retention indexes of the tumor and atelectasis were 29.7 and 42.0. The mean SUVs of FDG of the tumor and the atelectasis were 8.92 and 1.28. Tl-SPECT could not distinguish the atelectasis from the carcinoma. FDG-PET was superior to Tl-SPECT in this case in detecting malignancy and distinguishing it from atelectasis.

Key words: atelectasis, bronchogenic carcinoma, fluorine-18-fluorodeoxyglucose (FDG), thallium-201-chloride (Tl), retention index (RI)

INTRODUCTION

MANY REPORTS have revealed the usefulness of single photon emission computed tomography with thallium-201-chloride (Tl-SPECT)[1–3] and positron emission tomography with fluorine-18-fluorodeoxyglucose (FDG-PET)[4–7] for the diagnosis of bronchogenic carcinoma, but there is one report about a bronchogenic carcinoma with pulmonary atelectasis detected by Tl-SPECT[8] and no report by FDG-PET to our knowledge. We report a patient with bronchogenic carcinoma and pulmonary atelectasis examined by Tl-SPECT and FDG-PET. Tumor detection by the two techniques was compared, and the differences between the two in uptake in regions of atelectasis are discussed.

CASE REPORT

A 64-year-old man presented with a 2-month history of dyspnea and bloody sputum and was admitted to our hospital. Computed tomography (CT) with contrast material (Fig. 1) revealed a round and slightly enhanced mass which directly obstructed the left main bronchus, in a region of atelectasis in the left lung. An enlarged mediastinal lymph node and pleural effusion were also found.

Tl-SPECT was performed. A dose of 111 MBq of Tl was intravenously injected, and tomographic scans were obtained at 15 min (early image) and 3 hr (delayed image) post-injection with a three-headed gamma camera (TOSHIBA, GCA9300/HG). Early Tl-SPECT images revealed an oval-shaped region of high uptake in the left lung field and a hot spot in the mediastinum which was thought to be the enlarged mediastinal lymph node. Delayed Tl-SPECT images revealed that the high uptake in the left lung field was increased and wided, and the hot spot in the mediastinum was clearer than in the early image.

FDG-PET was performed for further examination. FDG was produced with the NKK-Oxford superconducting cyclotron and NKK synthesis system. A HEADTOME IV SET-1400W-10 (Shimadzu Corp., Japan), which has 4 detector rings providing 7 contiguous slices at 13 mm intervals, was employed for the PET study. Images were obtained from 40 to 55 minutes after intravenous injection of 370 MBq FDG while fasting. FDG-PET images revealed a round region of high uptake in the left lung and the hot spot in the mediastinum; the former region of high uptake was thought to be the primary tumor, and the latter the enlarged mediastinal lymph node.

To enable more concise comparison, the delayed

Received January 20, 1999, revision accepted April 12, 1999.

For reprint contact: Joji Kawabe, M.D., Division of Nuclear Medicine, Osaka City University, 1–5–7 Asahimachi, Abeno-ku, Osaka 545–8586, JAPAN.

E-mail: kawabe@msic.med.osaka-cu.ac.jp

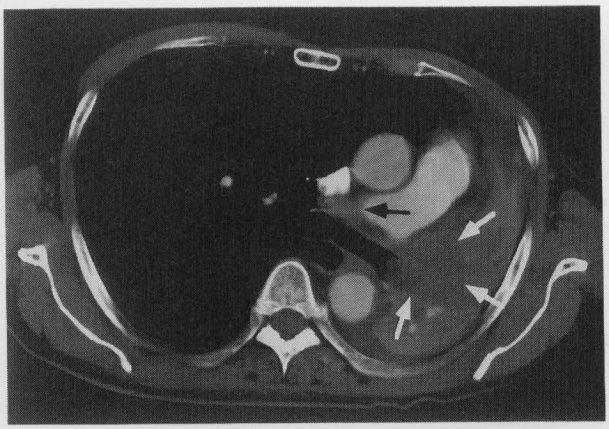

Fig. 1 Computed tomography (CT) with contrast material. A round and slightly enhanced mass (white arrow) that directly obstructed the left main bronchus in the region of atelectasis in the left lung, an enlarged mediastinal lymph node (black arrow), and pleural effusion are shown.

Tl-SPECT images and FDG-PET images were fused on the CT image with the same matrix size and the mediastinal lymph node as reference. The extent of abnormal FDG uptake was considered nearly equal to that of the tumor on the CT image (Fig. 2a), but abnormal uptake of Tl-SPECT was present not only in the tumor, but also in a portion of the collapsed lung surrounding the tumor on the CT image (Fig. 2b). FDG uptake in the region of atelectasis produced by the primary tumor was relatively low compared with that on Tl-SPECT. To compare the uptakes of Tl and FDG, regions of interest (ROIs: circles 3 pixels in diameter) were placed on the same locations in the early and delayed images of Tl-SPECT and FDG-PET images (Fig. 2c). On the Tl-SPECT images, early and delayed ratios[1] of ROIs (radioactivity of the lesion/radioactivity of the contralateral normal lung) were measured, and the retention index (RI) was then calculated to evaluate thallium retention in the lesions as follows: the difference between the delayed and early ratios was divided by the early ratio and expressed as a percentage.[1] On FDG-PET images, the standardized uptake values (SUVs; cpm per g tissue/cpm injected per g body weight) of ROIs were measured. The early ratios in the region of atelectasis (ROI 2,3) were 1.88 and 2.20 (average; 2.04), and in the tumor (ROI 4,5,6) 3.42, 3.68 and 3.16 (average; 3.42), respectively. The delayed ratios in the region of atelectasis (ROI 2,3) were 2.55 and 3.28 (average; 2.9), and in the tumor (ROI 4,5,6) 4.36, 4.47 and 4.26 (average; 4.4). RIs of the atelectasis (ROI 2,3) were 35, 49 (average; 42.0), respectively. RI of the tumor (ROI 4,5,6) were 27, 21 and 35 (average; 27.7), respectively. On FDG-PET, the mean SUVs for the region of atelectasis (ROI 2,3) were 1.24 and 1.32 (average; 1.28), for the contralateral normal lung (ROI 1) 0.28, and for the carcinoma (ROI 4,5,6) 7.58, 10.5 and 8.69 (average; 8.92).

A specimen of the tumor obtained by bronchoscopy was found to be poorly differentiated adenocarcinoma. After these examinations, the patient underwent left pneumonectomy. The primary tumor and the atelectasis surrounding the primary tumor are shown in Figure 3. On histopathologic examination, the tumor was found to be filled with tumor cells. The region of atelectasis has no tumor cell. Compared with the normal lung (Fig. 4a), the alveolar structure of the atelectatic lung (Fig. 4b) was collapsed and denser than that of the normal lung.

DISCUSSION

The usefulness of Tl-SPECT and FDG-PET for the diagnosis of bronchogenic carcinoma has been demonstrated in many reports.[1–7] Tonami et al.[1] found that the RI of Tl-SPECT is useful for detecting lung cancer and differentiating malignant from benign lesions. In their report, RI was 25 ± 24 in malignant lesions and 6 ± 24 in benign lesions. Suga et al.[2] found that RI was 23.3 ± 18.9 in malignant lesions and − 4.3 ± 13.6 in benign lesions. Gupta et al.[4] found that the mean SUV of FDG-PET of malignant pulmonary nodules was 5.63, whereas that of benign nodules was 0.56. Patz et al.[5] reported that the median SUV of bronchogenic carcinomas was 7.6, whereas that of fibrosis was 1.6. In our case the RI of Tl-SPECT of the carcinoma suggested malignancy, but the RI of the region of atelectasis was too high to deny malignancy. For FDG-PET, the average SUV of the region of atelectasis was low enough to distinguish it from the cancer. This indicated that FDG was much better for detecting malignancy and distinguishing it from atelectasis than thallium.

Concerning the mechanisms of Tl uptake, many theories, such as increasing blood flow,[9] sodium-potassium ATPase activation,[10,11] tumor viability and increased cell membrane potential[12] and others have been proposed. Tl accumulation in inflammatory or benign lesions decreases with time, but prolonged retention of radioactivity with delayed washout has been observed in malignant tumors.[1,2] Lee et al.,[8] however, demonstrated sustained retention of radioactivity within atelectasis for up to 4 hours in three of five patients. They assumed that Tl secreted into the interstitial space of the atelectatic lung was retained due to delayed lymphatic or venous drainage. Histopathological findings in our case indicated that the alveolar structure in the region of atelectasis of the resected lung was much denser than the normal alveolar structure of the resected lung. On FDG-PET, FDG uptake in the region of atelectasis was higher than that in the contralateral normal lung. Similarly, Tl uptake in the region of atelectasis was higher than that in the normal lung, probably reflecting the higher density in the region of atelectasis than in the normal lung. The increase in tissue density in our case appeared to be one of the reasons for the increase in Tl uptake in the region of atelectasis.

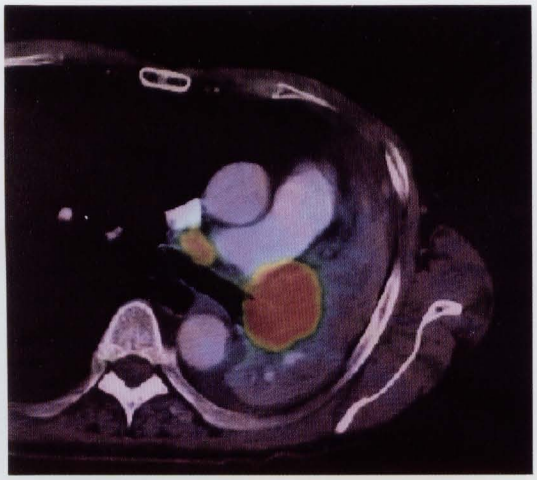

Fig. 2a FDG-PET image fused on CT image revealed a round region of high uptake in the left lung and the hot spot in the mediastinum; the former corresponded to the primary tumor, and the latter to the enlarged mediastinal lymph node. The extent of abnormal FDG uptake nearly equaled that of the tumor on the CT image.

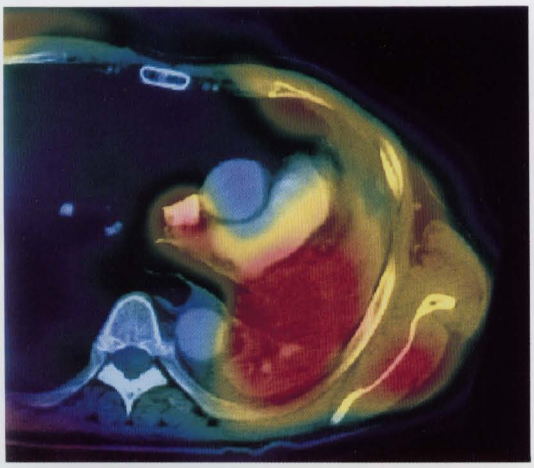

Fig. 2b Tl-SPECT image fused on CT image revealed an oval-shaped region of high uptake in the left lung field and a hot spot in the mediastinum, which corresponded to the enlarged mediastinal lymph node. Abnormal uptake in lung was found on the CT image not only in the tumor, but also in the collapsed lung surrounding the tumor.

Fig. 2c ROIs (circles: 3 pixels in diameter) were placed on the same locations in the Tl-SPECT and FDG-PET images.

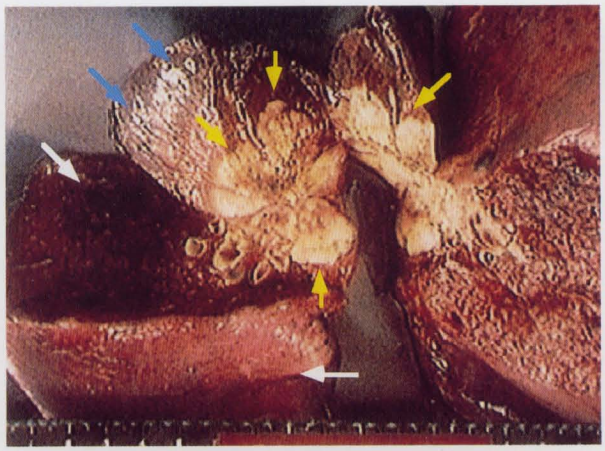

Fig. 3 The primary tumor (yellow arrow) and the region of atelectasis (blue arrow) surrounding the primary tumor are shown. The lower lobe (white arrow), which was found to be collapsed at operation, was expanded with air to enable comparison.

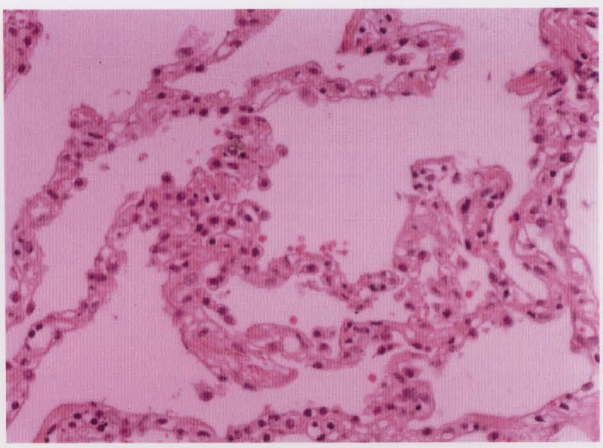

Fig. 4a Photomicrograph of the normal alveolar structure of the resected lung (hematoxylin-eosin stain; original magnification, × 20).

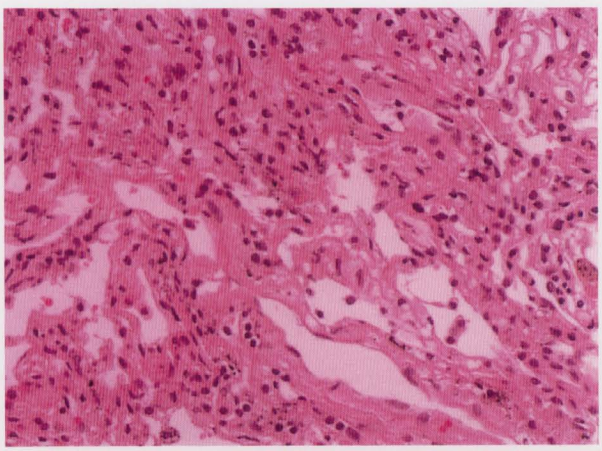

Fig. 4b Photomicrograph of the collapsed alveolar structure of the resected lung (hematoxylin-eosin stain; original magnification, × 20). In the region of atelectasis, the alveolar system was clearly collapsed and the structure was denser than that of normal alveoli.

REFERENCES

1. Tonami N, Yokoyama K, Shuke J, Taki S, Kinuya S, Miyauchi T, et al. Evaluation of suspected malignant pulmonary lesions with ^{201}Tl single photon emission computed tomography. *Nucl Med Commun* 14: 602–610, 1993.
2. Suga K, Kume N, Orihashi N, Nishiguchi K, Uchisako H, Matsumoto T, et al. Difference in ^{201}Tl accumulation on single photon emission computed tomography in benign and malignant thoracic lesions. *Nucl Med Commun* 14: 1071–1078, 1993.
3. Takekawa H, Takaoka K, Tsukamoto E, Kanegae K, Miller F, Kawakami Y. Thallium-201 single photon emission computed tomography as an indicator of prognosis for patients with lung carcinoma. *Cancer* 80: 198–203, 1997.
4. Gupta NC, Frank AR, Dewan NA, Redepenning LS, Rothberg ML, Mailliard JA, et al. Solitary pulmonary nodules: detection of malignancy with PET with 2-[F-18]-fluoro-2-deoxy-D-glucose. *Radiology* 184: 441–444, 1992.
5. Patz EF Jr, Lowe VJ, Hoffman JM, Paine SS, Harris LK, Goodman PC. Persistent or recurrent bronchogenic carcinoma: detection with PET and 2-[F-18]-2-deoxy-D-glucose. *Radiology* 191: 379–382, 1994.
6. Bury T, Dowlati A, Paulus P, Hustinx R, Radermecker M, Rigo P. Staging of non-small-cell lung cancer by whole-body fluorine-18 deoxyglucose positron emission tomography. *Eur J Nucl Med* 23: 204–206, 1996.
7. Sasaki M, Ichiya Y, Kuwabara Y, Akashi Y, Yoshida T, Fukumura T, et al. The usefulness of FDG positron emission tomography for the detection of mediastinal lymph node metastasis in patients with non-small cell lung cancer: a comparative study with X-ray computed tomography. *Eur J Nucl Med* 23: 741–747, 1996.
8. Lee JD, Lee BH, Kim SK, Chung KY, Shin DH, Park CY. Increased thallium-201 uptake in collapsed lung: a pitfall in scintigraphic evaluation of central bronchogenic carcinoma. *J Nucl Med* 35: 1125–1128, 1994.
9. Caluser C, Macapinlac H, Healey J, Ghavimi F, Meyers P, Wollner N, et al. The relationship between thallium uptake, blood flow, and blood pool activity in bone and soft tissue tumors. *Clin Nucl Med* 17: 565–572, 1992.
10. Sehweil AM, McKillop JH, Milroy R, Wilson R, Abdel Dayem HM, Omar YT. Mechanism of ^{201}Tl uptake in tumors. *Eur J Nucl Med* 15: 376–379, 1989.
11. Hanada T, Isobe H, Saito T, Ogura S, Takekawa H, Yamazaki K, et al. Intracellular accumulation of thallium as a marker of cisplatin cytotoxicity in non small cell lung carcinoma: an application of inductively coupled plasma mass spectrometry. *Cancer* 83: 930–935, 1998.
12. Brismar T, Collins VP, Kesselberg M. Thallium-201 uptake relates to membrane potential and potassium permeability in human glioma cells. *Brain Res* 500: 30–36, 1989.